Physics – Uspekhi **48** (3) 295 – 318 (2005)

CONFERENCES AND SYMPOSIA PACS number: 01.10.Fv

Joint scientific session of the Physical Sciences Division of the Russian Academy of Sciences and the Joint Physical Society of the Russian Federation 'Bose-condensation of excitons' (24 November 2004)

A joint scientific session of the Physical Sciences Division of the Russian Academy of Sciences (RAS) and the Joint Physical Society of the Russian Federation 'Bose-condensation of excitons' was held on 24 November 2004 at the Lebedev Physics Institute, RAS. The following reports were presented at the session:

(1) **Timofeev V B** (Institute of Solid-State Physics, RAS, Chernogolovka, Moscow region) "Collective exciton effects in spatially separated electron – hole layers in semiconductors";

(2) **Lozovik Yu E** (Institute of Spectroscopy, RAS, Troitsk, Moscow Region) "Coherence and superfluidity of excitons in two-dimensional systems and traps";

(3) **Gippius N A, Tikhodeev S G** (Prokhorov Institute of General Physics, RAS, Moscow), **Keldysh L V** (Lebedev Physics Institute, RAS, Moscow), **Kulakovskii V D** (Institute of Solid-State Physics, RAS, Chernogolovka, Moscow region) "Hard excitation of stimulated polariton – polariton scattering in semiconductor microcavities";

(4) **Kulakovskii V D, Krizhanovskii D N, Makhonin M N, Demenev A A** (Institute of Solid-State Physics, RAS, Chernogolovka, Moscow region), **Gippius N A, Tikhodeev S G** (Prokhorov Institute of General Physics, RAS, Moscow) "Stimulated polariton – polariton scattering in semiconductor microcavities".

An abridged version of reports 1, 3, and 4 is given below.

PACS numbers: 03.75.Nt, 71.35.Lk, 73.20.Mf
DOI: 10.1070/PU2005v048n03ABEH002123

Collective exciton effects in spatially separated electron – hole layers in semiconductors

V B Timofeev

1. Introduction

Excitons in a semiconductor are known to be the energetically lowest and electrically neutral excitations of electrons. Excitons have been used for several decades as a convenient tool to simulate the behavior of matter under the effect of density variation and external impacts, such as temperature, pressure, magnetic and electric fields, etc.

Uspekhi Fizicheskikh Nauk **175** (3) 315 – 340 (2005)
Translated by Yu V Morozov; edited by A M Semikhatov

Depending on the concentration of electron – hole (e – h) excitations and temperature, experiments with bulk semiconductors may be used to realize situations of a weakly interacting excitonic gas, molecular excitonic gas (biexcitonic gas), metallic electron – hole liquid, and electron – hole plasma.

An exciton consists of two fermions, an electron and a hole. This accounts for the resultant exciton spin being integer-valued and the exciton itself being a composite boson. This led to the hypothesis formulated in certain theoretical works in the early 1960s [1 – 3] that the Bose – Einstein condensation (BEC) is possible in a weakly nonideal and sufficiently dilute excitonic gas in bulk semiconductors at rather low temperatures (in the limit of rarified excitonic gas $na_{\rm ex}^d \ll 1$, where n is the exciton density, $a_{\rm ex}$ is the exciton Bohr radius, and d is the dimensionality of the system under study).

The Bose – Einstein condensation of excitons in three-dimensional systems suggests macroscopic occupation of the exciton ground state with zero momentum and the appearance of a spontaneous order parameter (coherence) in the condensate [4 – 6]. In the limit of high e – h density, $na_{\rm ex}^d \gg 1$, excitons used to be regarded in direct analogy to Cooper pairs, and the condensed excitonic state (or excitonic insulator state) was described in the mean-field approximation by analogy with the Bardeen – Cooper – Schrieffer superconducting state; the sole difference consisted in the fact that the pairing in an excitonic insulator was determined by the e – h interaction and the excitons themselves served as an analog of the Cooper pairs [4]. Well-apparent Coulomb gaps in the excitonic insulator state can arise under nesting of the electron – hole Fermi surfaces. Theoretical studies reported in Ref. [7] suggest a smooth transition between the low and high density limits.

The Bose – Einstein condensation in a weakly nonideal bosonic gas with a fixed density occurs when the critical temperature $T_{\rm c}$ is reached, which is inversely proportional to the Bose particle mass. BEC was recently discovered in the rarified and strongly cooled gases of atoms whose resulting spin is integer-valued [8 – 11]. This striking observation was possible owing to the elegant realization of the laser cooling technique in its application to rarified atomic gases and to the selective small-volume accumulation of atoms in magnetic traps. The transition temperatures $T_{\rm c}$ in alkaline atomic gases turned out to be very small (1 μK or lower), which is due to the large masses of atoms and their relatively low densities resulting from the inevitable losses during cooling and trapping.

After BEC had been found in the diluted gases of atoms and bosons, this phenomenon provoked special interest and

acquired significance with reference to excitons. The translational effective masses of excitons in semiconductors are typically small, i.e., equal to or smaller than the mass of a free electron. Therefore, unlike BEC in gases of atomic hydrogen, alkalis, and transition metals, BEC in an excitonic gas at experimentally achievable densities may occur at much higher temperatures (e.g., the temperature of liquid helium). However, excitonic gas being a photoexcitable and, in principle, nonequilibrium system, the problem of its cooling to temperatures of the crystal lattice serving as a thermostat assumes importance. Under real experimental conditions, the temperature of a quasi-equilibrium excitonic gas is always somewhat higher than that of the crystal lattice in which the excitons are 'immersed' due to their finite lifetime. Such overheating of the excitonic system is especially pronounced at $T < 1$ K because of the low thermal capacity of the lattice and the presence of a 'narrow' region at small transition momenta unsurmountable for the one-phonon relaxation of excitons ($\mathbf{K} < m\mathbf{s}/h$, where $\mathbf{K}$ and m are the exciton momentum and mass, respectively, and $\mathbf{s}$ is the speed of sound). In this context, the most promising objects in which to search for BEC are those whose exciton annihilation rate is several orders of magnitude lower than the exciton relaxation rate along the energy axis. This criterion is met, for example, by indirect-gap semiconductors in which radiative recombination of excitons involves short wavelength phonons and is therefore rather slow compared with relaxation processes that result in thermal equilibrium with the lattice. But because such semiconductors are characterized by strong orbital degeneracy of the electron (many valleys) and hole spectra and strong anisotropy of the effective carrier masses, the lowest state in an interacting and sufficiently dense e – h system is the electron – hole liquid into which excitons and excitonic molecules are condensed [12, 13]. The phenomenon of exciton condensation into droplets of the electron – hole fluid was predicted by L V Keldysh as early as 1968 [12] and most comprehensively studied in Ge and Si [13]. Evidently, a gas of excitons and excitonic molecules in equilibrium with the droplets of an e – h liquid remains a classical, Boltzmann gas. In contrast, the exciton recombination rates in direct-gap semiconductors with dipole-permitted interband transitions are very high. Moreover, other complications are intrinsic in such semiconductors related to the exciton – polariton dispersion and dynamics near $K = 0$ [14]. The peculiar properties of two-dimensional excitonic polaritons in microcavities and the related nonlinear optics and dynamics are considered at length in the reports by N A Gippius and co-workers and V D Kulakovskii and co-workers, published in this issue.

Some experiments have been designed to discover BEC in an excitonic gas in Cu_2O [15], where the ground state of para- and orthoexcitons is long-lived and forbidden in the zeroth order in K, and also in uniaxially deformed crystals of Ge [16] under conditions of broken symmetry with respect to the spin degrees of freedom. It was recently shown for Cu_2O that the Auger processes heat the excitonic system and restrict the exciton density from above [17]. For this reason, in optical pumping experiments conducted thus far, the excitonic gas in these crystals was the classical Boltzmann gas [17, 18]. Studies with Ge crystals examined excitons with the spin orientation, directly analogous to spin-aligned hydrogen atoms. The narrowing of the spontaneous exciton – phonon emission line with increasing concentration has evidenced the well-apparent degenerate Bose statistics of excitons at their high densities. But it is still impossible to realize the critical conditions for the BEC of excitons in the above crystals, although studies to this effect are underway.

In recent years, the BEC of excitons has been extensively sought in two-dimensional systems based on semiconductor heterostructures. The studies are focused on two-dimensional systems with spatially separated electron – hole layers. Researchers' attention to these objects was attracted by theoretical works done in the mid-1970s [19, 20]. In the context of the problem under consideration, double quantum wells (DQWs) and superlattices turned out to be the most interesting among quasi-two-dimensional objects based on semiconductor heterostructures because they allow the photoexcited electrons and holes to be spatially separated between adjacent QWs [21 – 32]. In DQWs to which a bias electric voltage is applied, it is possible to excite excitons whose electron and hole are in different QWs separated by a transparent tunnel barrier. Such an exciton is called a spatially indirect or interwell exciton (IWE), as opposed to a direct (D) or intrawell exciton in which the electron and the hole are located within the same QW (Fig. 1a). References [24, 25] report a situation realized in a GaAs/AlGaAs heterostructure where excitons are not only spatially separated but also prove to be indirect in momentum space. Interwell excitons have a longer lifetime than intrawell ones because of the limited overlap between the electron and hole wave functions through the tunnel barrier. Characteristic times of the radiative annihilation of IWEs are as large as dozens and hundreds of nanoseconds. Therefore, they are easy to accumulate, and the excitonic gas can be cooled to rather low temperatures close to the temperature of the crystal lattice. It is worthwhile to note that thermalization of two-dimensional excitons, such as interwell excitons, involves bulk phonons. In this case, however, the law of momentum conservation along the dimensional quantization axis is violated, which accounts for the lack of a 'bottleneck' for the transmission on small momenta and the feasibility of one-phonon relaxation with the participation of acoustic phonons at $T \leqslant 1$ K. As a result, the relaxation of IWE to the lattice temperature occurs a few orders of magnitude faster than their radiative decay [33, 34]. Because of the broken inverse symmetry, IWEs have a larger dipole moment even in the ground state. Such excitons cannot merge into molecules and larger complexes due to the dipole – dipole repulsion.

It should be recalled, however, that in an ideal and unconfined two-dimensional system with a constant density of one-particle states, BEC at finite temperatures cannot proceed in principle because of the divergence of the number of states in the case where the chemical potential $\mu \to 0$ (i.e., the states with momenta $\mathbf{K} \geqslant 0$ can accumulate an unlimited number of Bose particles). Therefore, in this case, one can speak about the Bose condensation only at $T = 0$ K, which has no physical sense. In this context, it is appropriate to recall work [35], which provides a rigorous proof (based on N N Bogolyubov's inequalities) that an unconfined and ideal two-dimensional system cannot have a nonzero order parameter (because it is destroyed by fluctuations). This proof is applicable to both superfluids and superconductivity in ideal two-dimensional systems. A similar theorem was proved for a two-dimensional model of Heisenberg's ferromagnet in [36]. The Kosterlitz – Thouless phase transition [37], during which the superfluid state in two-dimensional systems develops as a result of vortex pairing, is not discussed here. Such a transition is topological and not at variance with the theorem in Ref. [35].

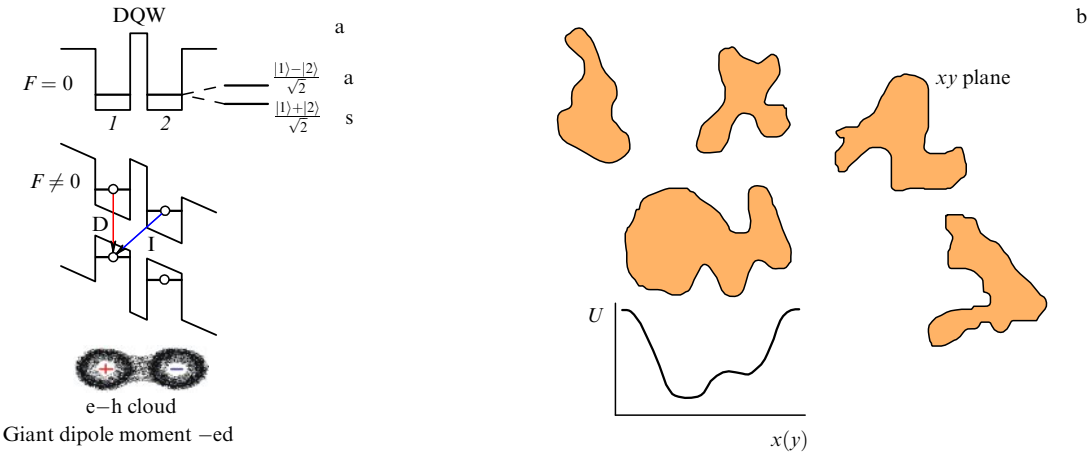

Figure 1. (a) Schematic representation of the energy levels in tunnel-linked DQWs in the absence, $F = 0$ (a — antisymmetric state, s — symmetric state), and in the presence, $F \neq 0$, of an electric field. Arrows indicate intrawell (D) and interwell (I) optical transition. The lower part of the figure qualitatively depicts the overlap between electron–hole clouds in an IWE. (b) Qualitative representation of a large-scale random potential and lateral trapping domains for interwell excitons.

Nevertheless, in quasi-two-dimensional and two-dimensional spatially confined systems, BEC is known to occur at finite temperatures. The critical temperature in a laterally confined two-dimensional system having a discrete spectrum and a finite number of states is given by the expression

$$T_c = \frac{2\pi\hbar^2 N_{ex}}{g_{ex} k_B m_{ex}} \ln \frac{N_{ex} S}{g_{ex}}, \qquad (1)$$

i.e., it decreases logarithmically with increasing the area S occupied by a two-dimensional gas of Bose particles with density N_{ex}, translational effective mass m_{ex}, and degeneracy factor g_{ex} (k_B is the Boltzmann constant). For example, the critical temperature T_c of an excitonic gas with the density 10^{10} cm^{-2} and translational mass of excitons $0.2m_0$ (m_0 is the free electron mass) under micron-scale lateral confinement is around 3 K.

The spatial confinement in the QW plane may be due to large-scale fluctuations in the random potential related to variations of the QW width on heteroboundaries $w(\mathbf{r})$. Also related to these variations are changes in the effective lateral potential $U(\mathbf{r}) = U\big(w(\mathbf{r})\big)$ [38]. Under quasi-equilibrium conditions, the exciton density distribution is described by the equality $\mu\big(N(\mathbf{r})\big) + U(\mathbf{r}) = \bar{\mu}$, where the chemical potential $\bar{\mu}$ of interwell excitons is related to their average density and $\mu(N)$ is the chemical potential of a homogeneous excitonic phase in the spatially confined domain. Evidently, $\big|\mu(\mathbf{r})\big| < |\bar{\mu}|$ because $\mu(N) = -|E_{ex}| + |\delta U|$ (E_{ex} is the exciton binding energy). This means that excitons more easily accumulate in the lateral confinement region, where their density can be much in excess of the mean density in the QW planes [38]. The critical conditions corresponding to the Bose condensation of IWEs are most readily realized in lateral domains that function as exciton traps. The qualitative form of the random large-scale potential and the related lateral trapping domains for IWE is depicted in Fig. 1b.

A variety of potential collective behavior scenarios in a sufficiently dense system of spatially separated electrons and holes were theoretically predicted in Refs [19, 20, 38–44]. For example, it was demonstrated in Ref. [42] that a liquid dielectric excitonic phase may constitute a metastable state in the e–h system despite the dipole–dipole repulsion of interwell excitons at certain critical parameters, such as the IWE dipole moment, density, and temperature. As shown in Ref. [38], the condensed dielectric excitonic phase (analog of the Bose condensate) can arise only in the presence of lateral confinement in the IWE plane (either spontaneous or artificially induced). Such confinement and the associated external compression facilitate the accumulation of interwell excitons to critical densities sufficient for the effects of collective exciton interactions to be manifested. Reference [41] discusses the role of spin degrees of freedom under Bose condensation conditions.

Real tunnel-linked quantum systems based on semiconductor heterostructures always include a random potential arising due to the presence of residual impurities, both charged and neutral, as well as a variety of structural defects. These imperfections create a random potential relief in IWE planes; as a result, photoexcited electrons and holes spatially separated between adjacent QWs (as well as IWEs) may be strongly localized on these fluctuations at sufficiently low temperatures. Such an effect of strong localization in coupled quantum systems is manifested, for example, as thermally activated tunneling of charge carriers [26, 27]. In connection with this, investigations into the properties of delocalized IWEs are carried out in structures with a minimum density of localized states ($\leqslant 10^9$ cm^{-2}) related to the chaotic potential that arises from the residual impurities.

2. Experimental

In this paper, we report a few recently conducted experiments using GaAs/AlGaAs heterostructures with DQWs (n–i–n structures) that have large-scale fluctuations in the random potential, where IWEs exhibit collective behavior after the critical density and temperature conditions are achieved [45, 46]. Double quantum wells 12 nm in thickness were separated by a narrow barrier of four AlAs monolayers. Similar AlAs epitaxial layers were grown on the borders between each QW and AlAgAs barrier. Large-scale fluctuations in the random potential were induced in these structures by the growth interruption technique on the boundaries of the AlAs and AlGaAs barriers. The architecture of the IWE-containing

heterostructures employed in these experiments is described at length in Refs [45, 46].

The main information about IWE properties has been obtained by the analysis of luminescence spectra measured as the excitation power, temperature, and polarization of the resonant optical pumping and magnetic field varied during steady-state or pulsed optical excitation.

2.1 Phase diagram

Figure 2 depicts luminescence spectra of IWEs measured at different biases. The optical transitions of interest are schematically presented in Fig. 1a. The intrawell luminescence region at zero electric bias exhibits two lines. One is 1sHH or the line of a free heavy-hole exciton (denoted as D) and the other is the line of a bound, charged excitonic complex (intrawell excitonic trion, T) [47]. At a small bias, it is possible to change both the charge and the structure of the excitonic trion by varying the sign of the gate voltage. The line of interwell excitons (I-line) emerges in the spectra after the electric field is switched on and causes the Stark shift of the dimensional quantization zones in adjacent QWs to be $eF\Delta z \geqslant E_D - E_I$ (E_D and E_I are intrawell and interwell exciton binding energies, respectively, F is the electric field strength, and Δz is the distance between the electron and the hole in the IWE). The I-line shifts almost linearly upon a change in the electric field at both positive and negative voltages between the electrodes (n^+-doped regions) (see the inset to Fig. 2). This line can be displaced along the energy scale over a distance almost ten times longer than the IWE binding energy. The asymmetry of the I-line shifts upon a change in the voltage sign due to the Schottky barrier at one of the electrodes. At high electric voltage and steady-state excitation, the IWE line in the luminescence spectra predominates. Under the same conditions, the luminescence of intrawell excitons (D) and charged excitonic complexes (T) is several orders of magnitude weaker. A large quantum yield of IWE luminescence in the studied structures suggests their high quality. This ensues from the fact that a rise in the applied bias causes the IWE lifetime to change by a factor of ten or more while the intensity of luminescence remains practically unaltered (see Fig. 2).

We consider changes in the IWE luminescence spectrum at various pumping values under a steady-state excitation by He – Ne laser radiation focused to form a spot of about 20 μm on the sample surface. The IWE luminescence line at sufficiently low temperatures ($T = 0.81$ K) and small pumping intensities around 100 nW is wide (≈ 2.5 meV) and asymmetric, with a large longwave 'tail' and clear-cut violet boundary (Fig. 3a). Such properties of the IWE photoluminescence line result from their strong localization on fluctuations of the random potential due to the presence of residual impurities. The line width then reflects the statistical distribution of the random potential amplitudes. As the pumping increases, a narrow (1.2 meV) line starts to emerge in a threshold manner at the blue end of the spectrum (see Fig. 3). The intensity of this line near the threshold grows superlinearly in accordance with a near-quadratic law (Fig. 3b). It is only at high-power pumping that the superlinear growth of the intensity changes into a linear one, and the line starts to broaden and extend towards higher energies. The shift of the line towards the high energies suggests screening of the applied electric field when the IWE density becomes sufficiently high. Then, the experimental measurement of this shift allows estimating the IWE density from

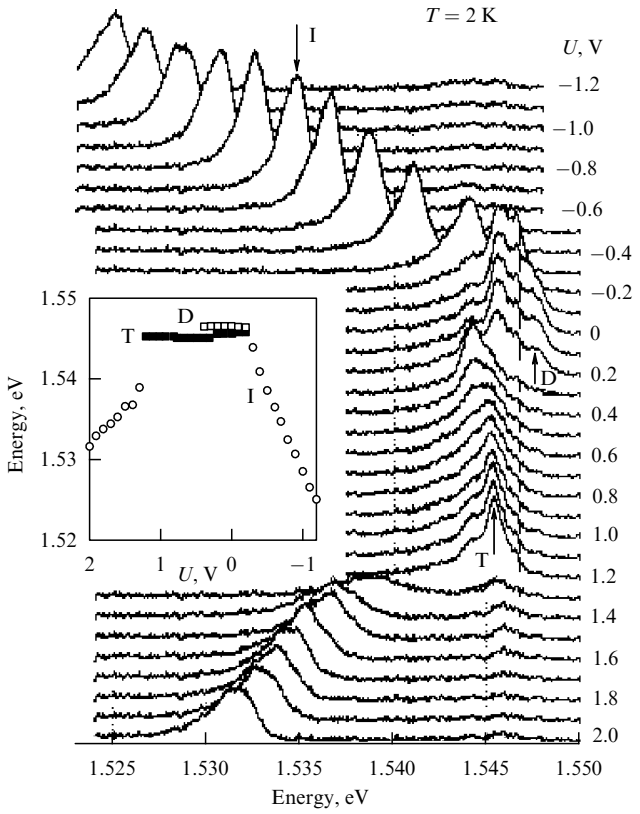

Figure 2. Luminescence spectra of intrawell excitons (D), trions (T), and interwell excitons (I) in DQWs at different bias voltages affecting dimensional quantization levels (U values in volts are given near the corresponding curves). The inset shows the dependence of spectral positions of the maxima on electric voltage. $T = 2$ K.

above using the Gauss formula for the spectral shift $\delta E = 4\pi e^2 n \Delta Z/\varepsilon$ (n is the exciton density, ΔZ is the distance between the electron and the hole in an exciton, and ε is the dielectric permittivity). With this approach, the IWE concentration is $n = 3 \times 10^{10}$ cm^{-2} when the line is shifted by less than 1.3 meV. A sufficiently narrow IWE luminescence line can be seen at various negative bias voltages in the range from -0.5 to -1.2 V. A similar narrowing of the IWE luminescence line at larger negative voltages occurs at much smaller pumping intensities.

Studies on the behavior of the narrow IWE luminescence line at different temperatures have demonstrated that it disappears from the spectrum at $T \geqslant 5$ K. Figure 4 illustrates the typical behavior of the I-line at different temperatures and fixed pumping intensities. It can be seen that at $T = 1.64$ K and excitation power 2 μW, this high-intensity line evidently rises above the structureless luminescence band of localized excitons. Its intensity drops with increasing the temperature without a change in the width; at $T = 4.2$ K, the I-line becomes practically indiscernible against the background of the structureless spectrum of localized excitons, which retains its shape. It is worth noting that a decrease in the intensity of the I-line with increasing the temperature has no activating character and obeys a close-to-linear power law.

Direct evidence of the IWE condensation was obtained in experiments with single trapping domains associated with large-scale fluctuations of the random potential. The experiments were conducted using n–i–n structures of the described architecture covered with a 100 nm thick metallic

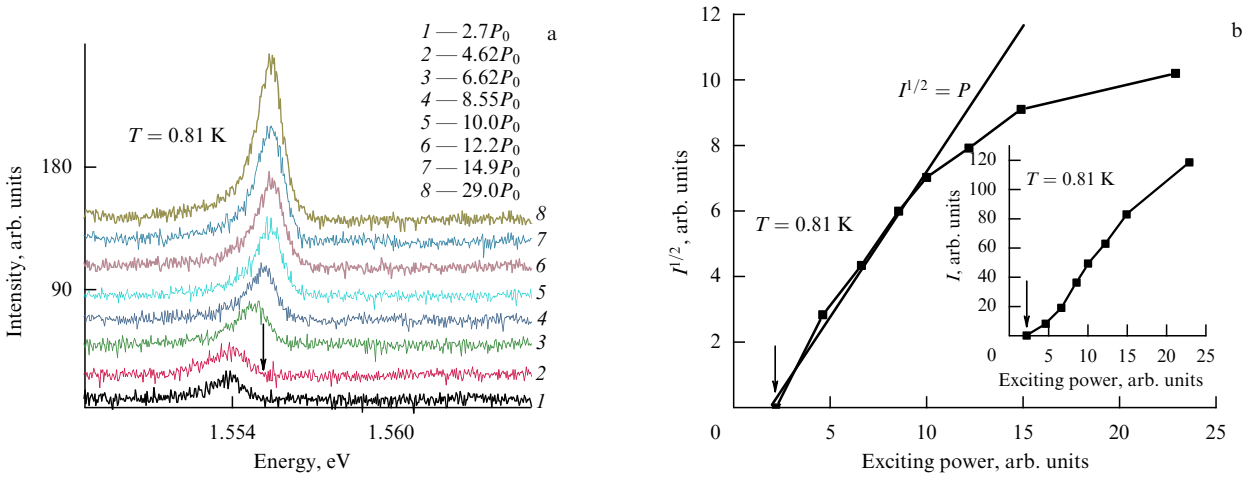

Figure 3. (a) Luminescence spectra at growing excitation power, $P_0 = 60$ nW, $T = 0.81$ K. (b) Intensity of the narrow line of interwell excitons plotted versus the exciting power P. The arrow indicates the threshold pumping value (~ 200 nW) after which the narrow line becomes apparent in the spectrum.

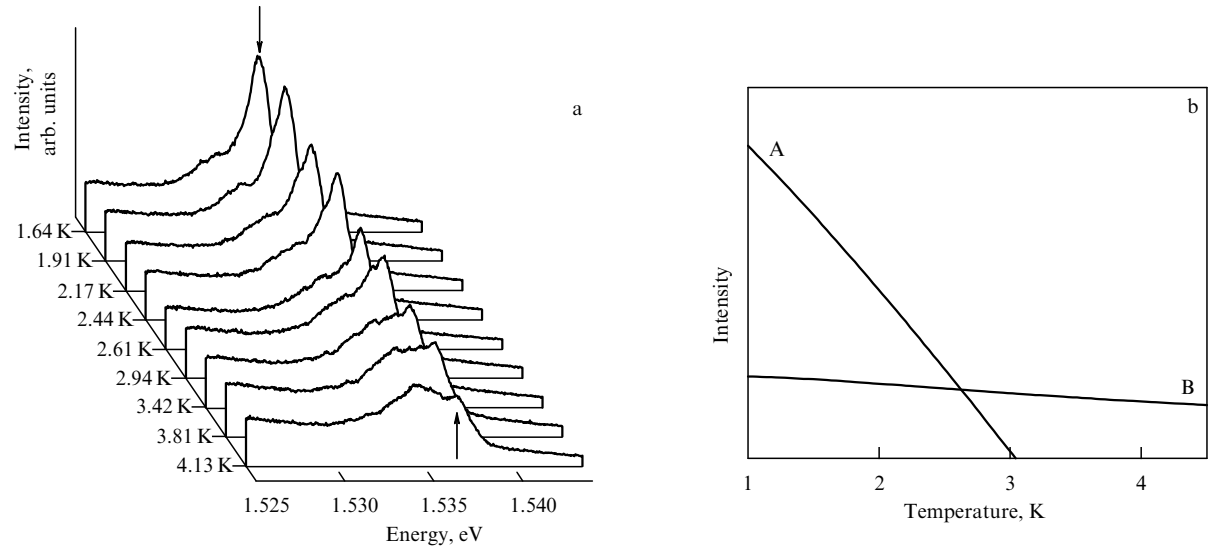

Figure 4. (a) Temperature dependence of the luminescence intensity of the IWE condensate. (b) Computed temperature dependences of the luminescence intensities of condensed interwell (A) and supracondensate (B) excitons.

layer (aluminum film). The film was etched using electron-ray lift-off photolithography to fabricate annulus-shaped holes with a minimum diameter around 0.5 μm. These holes were used to excite and record luminescence signals. The aluminum film was not in contact with the n^+-doped contact region of the heterostructure.

The results expounded below were obtained by optical excitation of the sample and subsequent detection of luminescence directly through holes about 1 μm in diameter (Fig. 5). The experiments were carried out under resonant excitation of intrawell excitons with heavy holes (1sHH-excitons) by a tunable Ti–Sp laser in order to minimally overheat the excitonic system relative to the lattice temperature. At small excitation densities (below 40 μW), the luminescence spectra exhibit a relatively wide (some 2 meV) asymmetric IWE band (Fig. 5a). This irregularly broadened band is due to the strong localization of IWEs in small-scale fluctuations of the random potential associated with the residual charge impurities. As the pumping increases ($\geqslant 50$ μW), a narrow line emerges in a threshold manner at the blue end of the broad band. The intensity of this line grows superlinearly with increasing pumping (see the inset to Fig. 5a), slightly narrowing and shifting by approximately 0.5 meV towards smaller energies. The minimal measured total width of this line in the experiments was about 300 μeV. It was close to the lattice temperature but somewhat higher than that. A further rise in pumping intensity (to over 0.5 mW) led to a monotonic broadening of the narrow IWE line and its shift towards higher energies (the external electric field screening effect).

In this experiment, the narrow IWE line disappeared from the spectrum at temperatures $T \geqslant 3.6$ K. Figure 5b illustrates the typical behavior of the I-line upon temperature variations and fixed pumping. It can be seen that at $T = 1.8$ K and the excitation power 250 μW, this high-intensity line evidently rises above the structureless luminescence band of localized excitons. Its intensity drops with increasing the temperature without a substantial change in the width; at $T = 3.6$ K, it becomes practically indiscernible against the background of the structureless spectrum of localized excitons, which retains

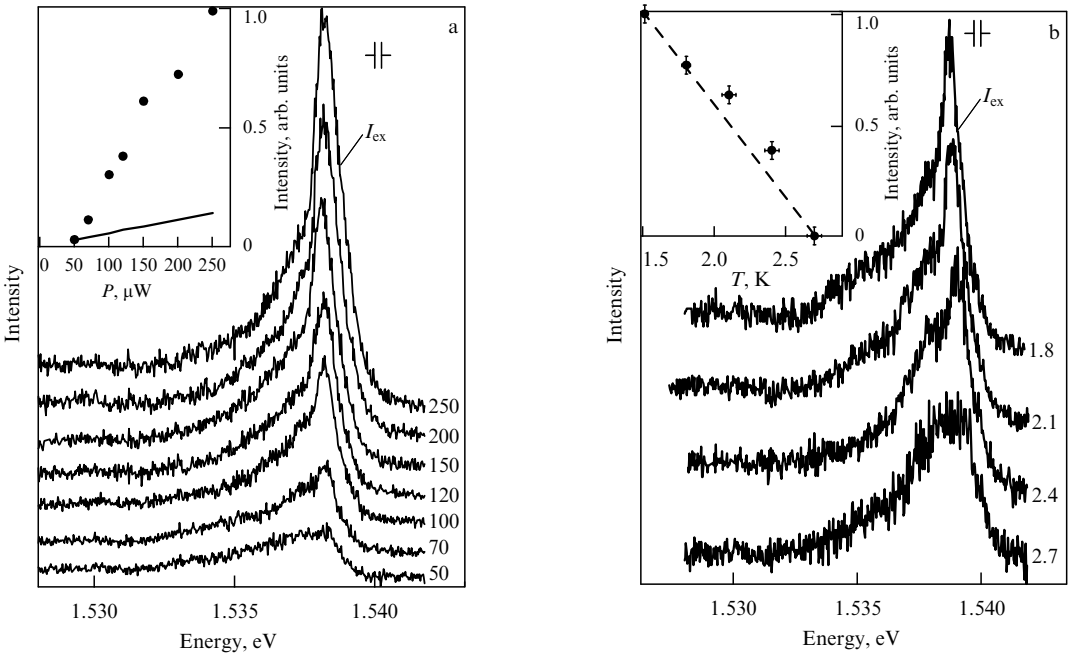

Figure 5. IWE luminescence spectra in a sample coated with a metallic film detected through micron-scale windows: (a) at various excitation power values given near the corresponding curves in microwatts ($T = 1.6$ K); (b) at various temperatures, shown to the right of the corresponding curves in kelvin.

its shape. It is noteworthy that a decrease in the intensity of the I-line with increasing temperature is not of the activating nature. Measurements of the temperature dependence of the I-line intensity in different pumping regimes yielded the following relation for its temperature dependence:

$$I_T \propto 1 - \frac{T}{T_c}\,, \tag{2}$$

where I_T is line intensity and T_c is the critical temperature corresponding to the disappearance of this line from the spectrum at a given fixed pumping.

We believe that the above experimental findings are evidence of the Bose condensation of IWEs in a single lateral domain about 1 μm in size that originates from large-scale fluctuations in the random potential. At small pumping intensities and sufficiently low temperatures, the photoexcited IWEs turn out to be strongly localized due to the presence of small-scale imperfections (e.g., residual charged impurities). Corresponding to this situation is a wide, irregularly broadened luminescence band of IWEs at small excitation densities. A strong dipole–dipole repulsion precludes localization of more than one exciton on a defect. This accounts for the quick saturation of this luminescence channel observed in the above experiments at concentrations below 3×10^9 cm^{-2}. A further, above-threshold increase in the pumping intensity in the domain results in the delocalization of IWEs. After the critical density values are reached, excitons undergo condensation to the lowest delocalization state. In experiments, this transformation is apparent as the appearance, in the threshold manner, of a narrow luminescence line, its further narrowing with a rise in pumping, superlinear growth, and displacement towards lower energies in accordance with the filling of the lowest state in the domain by excitons that obey the Bose–Einstein statistics. The most convincing argument in favor of the exciton condensation is the critical temperature dependence of their properties. It is possible to calculate the change in the luminescence intensity of the condensed and supracondensate fractions of the excitons in a micron-scale trapping domain as the temperature increases. The results of such calculations are presented in Fig. 4b [48]. It can be seen that in the framework of the model used, Ref. [48], the linear behavior of the intensity of the narrow luminescence line at varying temperatures, up to its disappearance from the spectrum, is realized only for condensed excitons. At the same time, luminescence of supracondensate excitons displays very low sensitivity to temperature variations in the range under study.

We evaluated the threshold for the appearance of the narrow IWE luminescence line corresponding to the onset of macro-occupation by excitons of the lowest state in the lateral trapping domain. The results were used to construct a phase diagram outlining the region of the excitonic Bose condensate (Fig. 6). For this, we examined pumping dependences of the luminescence spectra in the temperature range 0.5–4 K. For each temperature value in this range, we determined the threshold powers P_c at which the narrow spectral line corresponding to the excitonic condensate either appeared for the first time or began to disappear. In other words, the phase diagram was built in the coordinates $P_c - T$. The density of interwell excitons was estimated from the 'violet' shift of the line associated with the screening of the applied electric voltage at large pumping intensities. The threshold exciton density thus found was $n_c = 3 \times 10^9$ cm^{-2} at $T = 0.55$ K (indicated by the arrow in Fig. 6). The line intensities and exciton densities on the pump scale of the phase diagram were linearly related. In the temperature range 1–4 K, the critical density and temperature values at which condensation occurs are related by the power law

$$N_c \approx T^{\alpha}\,, \tag{3}$$

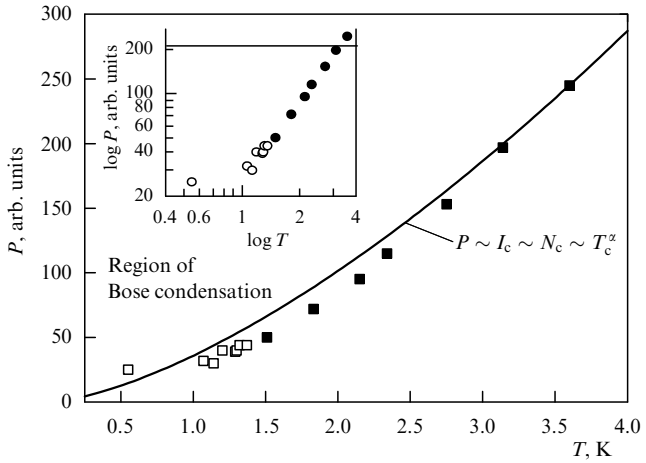

Figure 6. Phase diagram of the Bose condensation of interwell excitons in samples with large-scale fluctuations of the random potential. Open squares and circles correspond to optical excitation by a Ti–SP laser, black ones to that by an Ne–He laser.

where $\alpha \geqslant 1$. At $T < 1$ K, the phase boundary cannot be described by a simple power law.

2.2 Coherence of excitonic condensate

Condensed excitons must be spatially coherent. The spatial coherence must be manifested at least on the scales of the de Broglie IWE wavelength $\lambda_{ex} \approx h/\sqrt{\pi m_{ex} kT} = 1.5 \times 10^3$ Å, at $T = 2$ K, which is one order of magnitude larger than the exciton Bohr radius. The exciton density in the above experiments corresponded to the dimensionless parameter $r_\lambda = n\lambda_{ex}^2 = 4$. At such spatial scales, coherent excitons must be phased, i.e., described by the same wave function. The development of a collective excitonic state may be accompanied by a rise in the radiative decay rate of condensed excitons compared with that of supracondensate ones, as well and by a longer spin relaxation time of condensed excitons than one-particle excitonic spin relaxation.

These hypotheses were verified in experiments on the resonant excitation of excitons by polarized light. We recall that the ground state of IWEs is not a simple Kramers doublet but is quadruply degenerate with respect to angular momentum projections ($M = \pm 1, \pm 2$). Bright and dark excitonic states are characterized by the respective angular momentum projections $M = \pm 1$ and $M = \pm 2$. In the case of the resonant steady-state excitation of intrawell 1sHH excitons by circularly polarized light, the degree of circular polarization of the narrow IWE line corresponding to the condensed phase was found to increase in a threshold manner (Fig. 7). Enhanced pumping caused a rise in the degree of polarization up to 40%. This effect indirectly evidenced a rise in the radiative exciton recombination rate in the condensate and a possible increase in the spin relaxation time. Both were confirmed by direct measurements of the evolution and kinetics of the luminescence spectra under conditions of pulsed resonant excitation by circularly polarized light (Fig. 8). It follows from Fig. 8a that the narrow line of the condensed excitonic phase emerged in the spectra when the pulsed excitation was applied with a delay of about 4 ns. Its decay time was 20 ns, whereas the continuum under the narrow line 'lived' over 100 ns. Direct measurements of the circular polarization degree demonstrated that the spin relaxation time of condensed excitons was almost twice as long as the one-particle

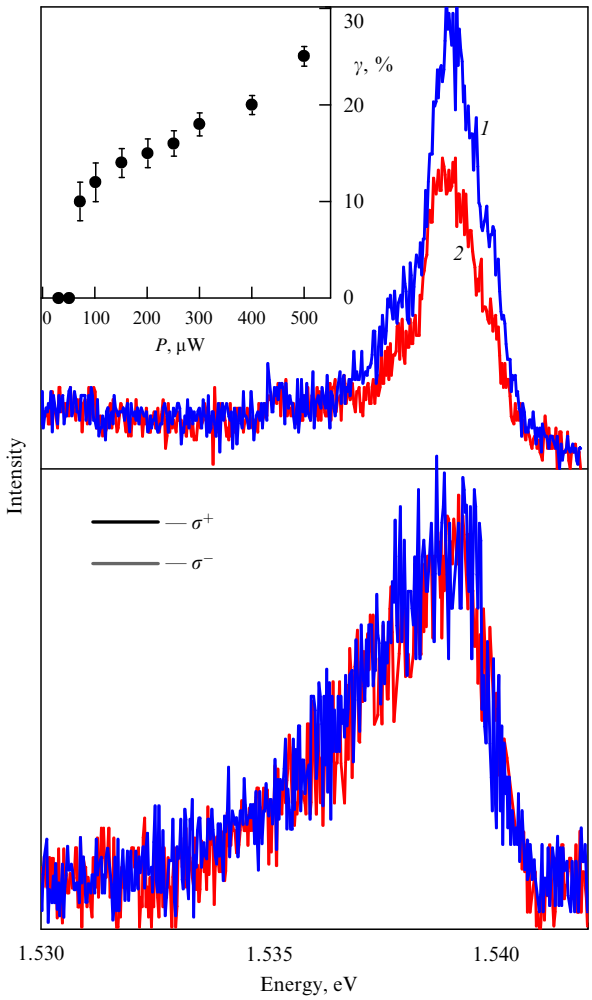

Figure 7. Luminescence of interwell excitons resonantly excited by circularly polarized light. Curves *1* and *2* in the top figure correspond to the clockwise and counterclockwise polarization, respectively (excitation power 150 μW). The luminescence line in the bottom figure (excitation power 60 μW) is not polarized: line contours measured for clockwise and counterclockwise polarization are indiscriminable within the measured noise range. The inset shows the excitative power dependence of the circular polarization degree γ of the IWE luminescence line.

excitonic relaxation measured at $T > T_c$ (Fig. 8b). These results may be regarded as indirect evidence of the enlarged coherent volume of excitonic condensates.

In considering the enhanced coherence of the condensed excitonic phase, one cannot disregard the interesting experiments of Butov and co-workers [29, 31] in which the authors observed an unusual behavior of IWE photoluminescence kinetics following pulsed laser excitation. At sufficiently large excitation powers and low temperatures, the kinetics of the IWE radiative decay cannot be described by a simple exponential law. Instead, the intensity of photoluminescence increases in a jump immediately after the pulse and thereafter decreases nonexponentially rapidly.

Such unusual behavior of radiative decay kinetics cannot be observed at a small excitation power, at high temperatures, during strong disorder associated with a chaotic potential, or in the presence of a magnetic field perpendicular to the heterolayers. Under such conditions, the photoluminescence kinetics is monoexponential and characterized by large times. We must note that only those delocalized excitons whose

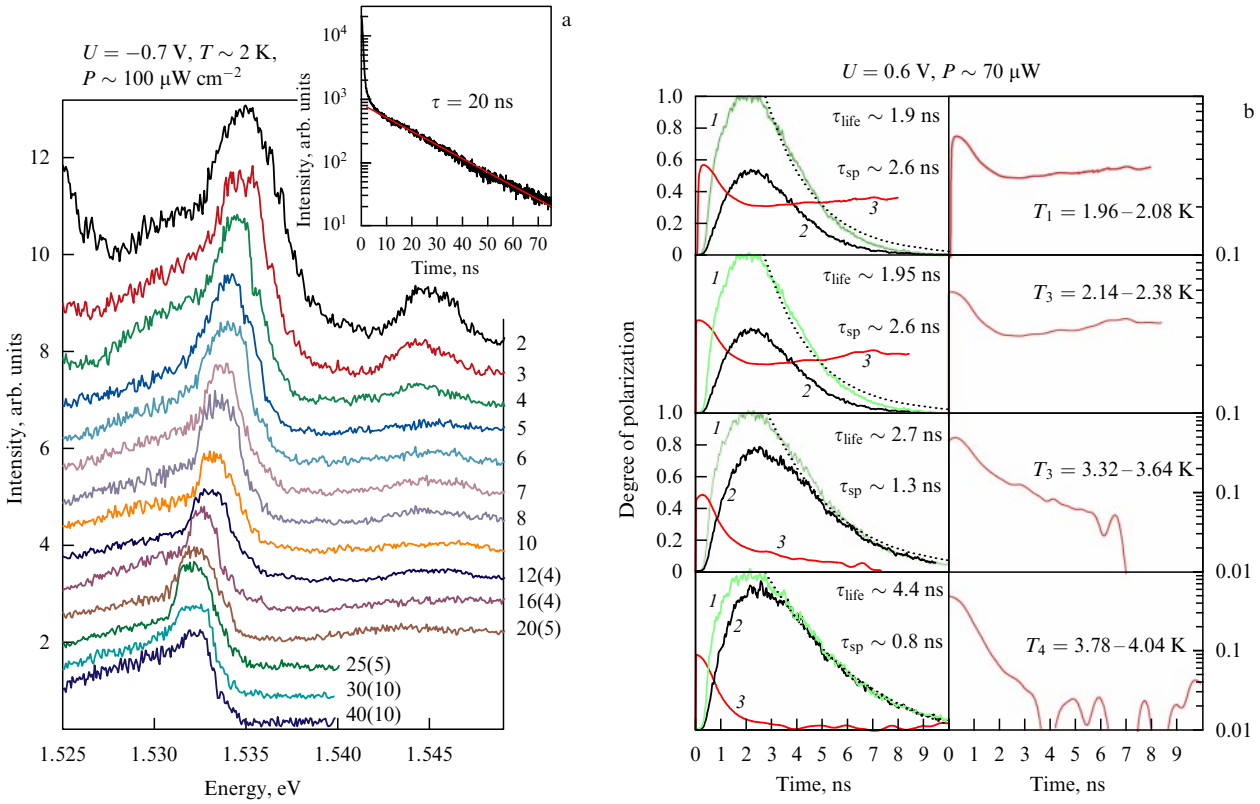

Figure 8. (a) Time evolution of IWE luminescence spectra under pulsed excitation conditions. Figures to the right of the curves are the delay times and signal integration times (in parentheses) in nanoseconds. The potential U of the n–i–n structure with DQWs equals -0.7 V. The inset shows IWE luminescence decay kinetics. $T = 2$ K. (b) Kinetics of circularly polarized IWE luminescence and its degrees of circular polarization under pulsed resonant excitation by circularly polarized light. The measured degree of circular polarization is given for each kinetic picture in the left part; measured temperature intervals are shown in the right part; τ_{life} is the lifetime of IWEs; τ_{sp} is the IWE spin relaxation time. Curves *1* and *2* correspond to positive and negative circular polarization, respectively; curve *3* shows the circular polarization degree. The dependence of the circular polarization degree of the luminescence line in the right part is given in a logarithmic scale.

translational motion momenta are of the order of the light momentum undergo radiative annihilation, i.e., $K \leqslant E_g/hc$ (c is the speed of light). The rise in the IWE radiative annihilation rate observed in Refs [29, 31] is regarded by the authors as a result of two effects. One is related to the enlargement of the IWE coherence area under conditions of the exciton condensation to states with smaller momenta than the light ones. The other is assumed to be due to the superlinear filling of the optically active excitonic states induced by the stimulated exciton scattering, when the filling numbers in the final exciton state $n \gg 1$ (i.e., as a result of the degenerate Bose statistics of IWEs).

The development of the collective excitonic state in our case is also confirmed by experiments in a magnetic field transverse to the electron–hole layers. Effects of magnetic fields on intrawell and interwell excitons are analyzed in detail in the studies by Lozovik, Butov et al. [31, 54–56]. On the one hand, the action of a transverse magnetic field on IWEs eliminates degeneracy with respect to spin degrees of freedom and increases the exciton binding energy. On the other hand, it causes the enlargement of the translational exciton mass. In the limit where the magnetic length exceeds the difference between the electron–hole layers, $l_B > \Delta Z$, the translational mass of IWE increases, i.e., $m_{ex} \propto \sqrt{B}$. Therefore, the magnetic field finally 'suppresses' exciton condensation. It follows from Fig. 9 that the intensity of the condensed part of IWEs significantly decreases as the transverse magnetic field grows.

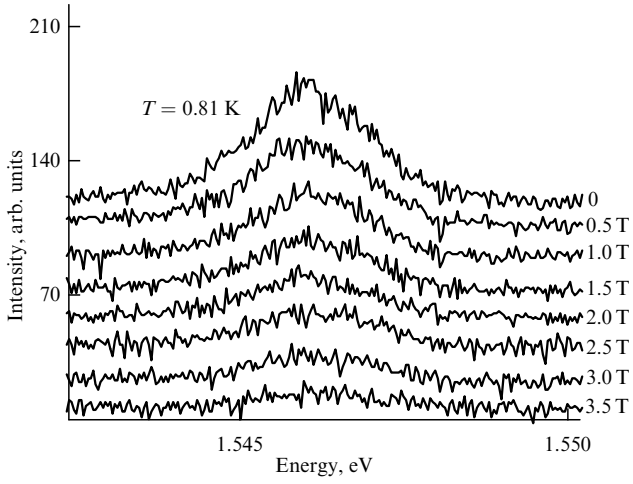

Figure 9. Luminescence of the IWE condensate in a magnetic field transverse to the layers. Figures to the right of the curves are magnetic field strengths. The magnetic field suppresses the intensity of luminescence of condensed excitons.

2.3 Condensation of interwell excitons in a nonuniform electric field

In the case of lateral traps due to a large-scale chaotic potential, the potential well shape, the actual depth, and the lateral dimension remain to be determined; this leads to the acute problem of artificially creating lateral traps for IWEs

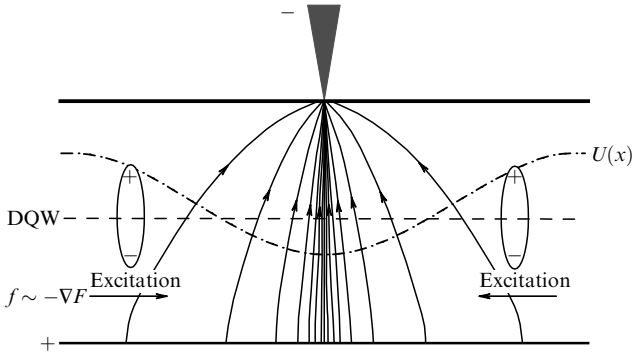

Figure 10. Schematic representation of a nonuniform electric field in a DQW-containing heterostructure when the current runs through the point contact into the bulk of the structure. The arrows are electric field lines close to the needle; the dashed-dotted line shows the potential well for excitons; the dashed line is the DQW cross section.

by means of controlled external impacts, with properties amenable to reliable management and monitoring. Nonuniform electric fields appear to be most suitable for the purpose. The action of such fields on excitons is schematically illustrated by Fig. 10. As the current flows through the point contact between the needle of a tunneling microscope and the surface of a DQW-containing heterostructure, with a bias electric voltage applied between the conducting needle and the in-built gate, it generates a strongly nonuniform electric field. Naturally, the maximum field strength can be expected to be found directly beneath the needle tip. It can be monitored experimentally from the spectral shift of the IWE luminescence band with respect to the intrawell exciton line.

Furthermore, IWEs are dipoles. When placed in a nonuniform electric field, they are subject to the action of electrostatic forces, $f \approx -e\nabla F$, which make them move to the center of the potential well functioning as a IWE trap. The distance over which the excitons can drift depends on the field gradient, exciton lifetime, and mobility. The qualitative aspect of the potential well in Fig. 10 is depicted by the dashed-dotted line.

The nonuniform electric field inside the heterostructure was created using the needle of a tunneling microscope as schematically shown in Fig. 10. A commercial silicon cantilever of the tunneling microscope was used for the purpose. The cantilever bearing a needle covered with a 120 nm thick gold film was mounted on a pair of bimorphic piezoceramic plates fastened together. The construction ensured a 'soft' touch of the needle with the sample surface when an electric voltage was applied to the piezoceramic plates. The entire device was placed in liquid helium inside an optical cryostat [49].

We consider the shape that the potential well had when the current flowed through the above structure. For this, the exciton luminescent spectra were measured with regard to the position of the finely focused spot (about 20 μm in size) of luminescence-exciting laser light relative to the point contact (Figs 11 and 12) [49]. The luminescence was detected directly inside the exciting laser spot. This region was singled out using special diaphragms and projected onto the entrance slit of the spectrometer. Figures 11 and 12 show the luminescence spectra of interwell and intrawell excitons depending on the distance from the point contact. The figures also illustrate the

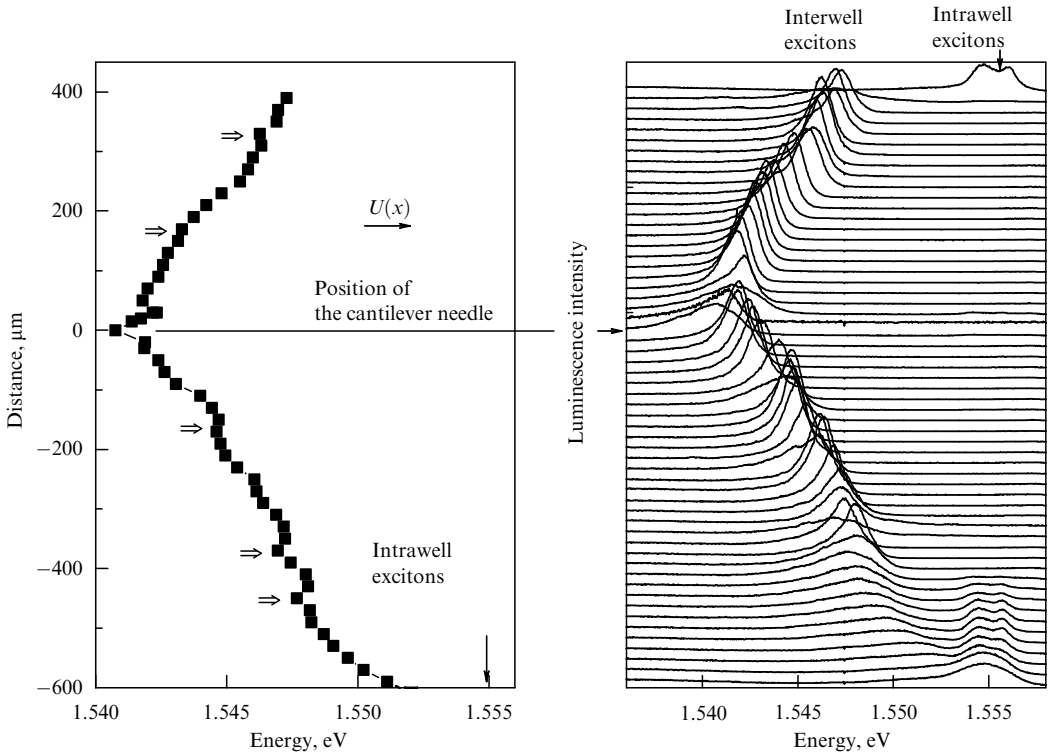

Figure 11. Profile of the lateral potential well created by a nonuniform electric field. The right part of the figure shows the luminescence spectra of interwell and intrawell excitons measured at different distances between the exciting laser spot and the point contact (the focused spot size is around 20 μm, the luminescence is detected only from the excitation region). The left figure shows the position of the IWE luminescence maximum depending on the same distances. $T = 2$ K.

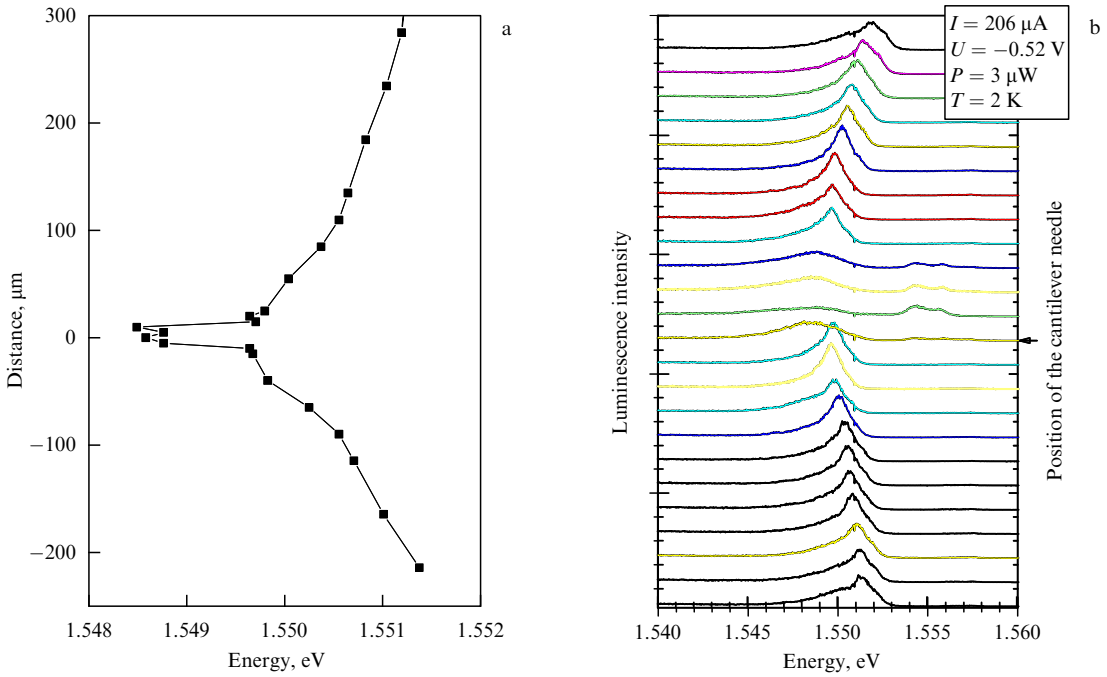

Figure 12. Lateral potential well created by a nonuniform electric field close to the cantilever needle: (a) position of the IWE luminescence maximum measured at different distances between the exciting laser spot and the point contact; (b) luminescence spectra of interwell and intrawell excitons depending on the same distances.

behavior of the spectral position of the luminescence maxima of interwell excitons as a function of the same distance. These figures essentially depict the shape of the lateral potential well for IWEs: $U(x) \simeq eF(x)\Delta Z + E_{\mathrm{I}}(x)$. It can be seen that the largest spectral shift in IWE luminescence relative to the line of intrawell excitons occurs in the immediate proximity of the point contact, where the well has the largest depth (see Fig. 12) and the spectral shift amounts to 13.5 meV at the current 27 μA passing through the entire structure. This shift is a good indicator of the maximum electric field strength, which equals 1.1×10^4 V cm^{-1} in the case under consideration. It decreases with the distance from the point contact, and the intrawell exciton spectral line begins to appear at distances of the order of 500 μm.

The above electric field distribution around the point contact is close to an axially symmetric one, but the radial distribution of the electric potential is not a monotonic function of the distance from the contact. First, the potential well shows a deep and narrow gap in the immediate proximity to the contact (see Fig. 12). The most surprising and unexpected finding is that such narrow and rather deep gaps in the potential curve are located far from the center of the well (as shown by the wide arrows in the left part of Fig. 11). These narrow falls always occur when the current exceeds 1 μA and depart from the well center as the current grows further. The origin of such axially positioned falls on the potential curve awaits explanation. They may result from the nonlinear screening of the electric field by photoexcited carriers inside the structure. However, narrow gaps in the potential curve can by themselves function as lateral traps for IWEs. Here, a special note is in order to the effect that the falls in question on the potential curve have a different origin unrelated to the nature of IWE luminescence that manifests itself in the form of narrow lateral rings similar to those observed in experiments by Butov et al. [50, 51] and in Refs [52, 53]. Such circular luminescence structures arose

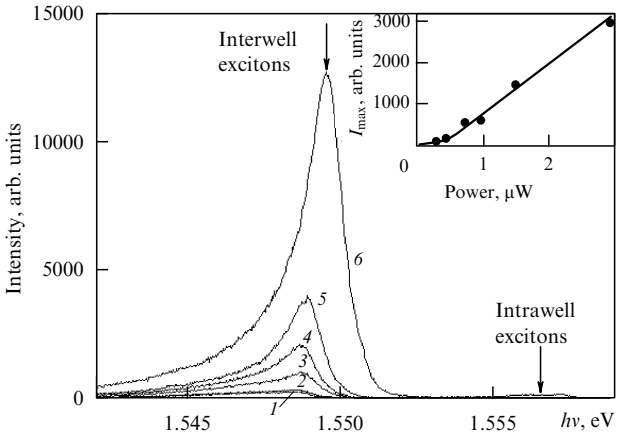

Figure 13. IWE luminescence spectra upon variations in the exciting power measured directly out of the potential well created by a nonuniform electric field and spaced 80 μm from the needle. The inset shows the power dependence of the maximum intensity $I_{\max}$. $T = 2$ K.

under the effect of rather powerful focused laser radiation. Their origin is related to the depletion of electrons and field screening in the optical pumping region, as well as to the oncoming drift of electrons and holes that occurs under these conditions.

Of interest is the behavior of the IWE luminescence excited directly in the traps created by a nonuniform electric field. A wide IWE luminescence band (about 2–3 meV) is produced in the central trap located just beneath the needle due to the strong overheating of the near-contact region with the maximum current density (see Fig. 12). Also interesting in this context are the falls on the potential curve located far away from the contact site, in which overheating can be neglected. These regions are also potential traps for IWEs. Therefore, it is worth examining exciton luminescence excited

in one of the traps remote from the center (Fig. 13). Weak pumping (below 300 nW) induces a wide asymmetric band in the IWE luminescence spectrum (bandwidth around 3 meV) with a longwave 'tail', whose intensity gradually decreases. This irregularly broadened band is due to the radiative decay of strongly localized excitons. At a pumping power in excess of 300 nW, a rather narrow line of delocalized excitons arises in a threshold manner at the blue end of this band. Its intensity near the threshold behaves superlinearly as the pumping increases. Only at large pumping powers of more than 3 μW does the IWE luminescence band begin to broaden and shift towards higher energies due to the electric field screening. As the excitation power varies, the behavior of the IWE spectra in lateral traps 'prepared' by the electric field is qualitatively similar to the behavior of IWEs during their condensation to the lowest state in the lateral trapping domains associated with large-scale fluctuations of a random potential.

3. Conclusion

The phenomenon of Bose condensation discovered in the studied structures emerges in a limited range on the exciton concentration scale: $N_{\rm loc} < N_{\rm ex} < N_{\rm I-M}$. In the low-density region ($N_{\rm loc} \leqslant 3 \times 10^9$ cm^{-2}), the limitation is imposed by effects of strong exciton localization on imperfections and in the high-density region ($N_{\rm I-M}$), by the exciton decay caused by the insulator–metal transition. Indeed, a rise in the excitation power above 0.5 mW leads to the broadening of the IWE luminescence line in our structures, which continues to be extended and shifts to the region of large energies. The broadening of the I-line results from the overlap between the exciton wave functions in the QW planes and the associated Fermi repulsion between electrons in one well and holes in another. At an estimated density $N_{\rm I-M} \simeq 8 \times 10^{10}$ cm^{-2}, interwell excitons lose their individual characteristics and the e–h plasma is formed, with electrons and holes spatially separated between adjacent QWs. Corresponding to this density is the dimensionless parameter $r_S = 1/(\pi N_{\rm I-M})^{1/2} a_{\rm B} = 1.8$ (the excitonic Bohr radius $a_{\rm B} \approx 150$ Å was found from the diamagnetic shift of IWEs). The e–h plasma begins to screen the externally applied electric field, and the interwell recombination band shifts towards large energies. It is this shift that was used to find the e–h density. It is also worth noting that the total number of condensed excitons in experiments with micron-scale domains was close to 10^2.

Nevertheless, the substantiation of the conjectural condensation of IWEs to a dielectric collective phase lacks a definitive answer to the important unsolved question about the spatial coherence scale of this collective state. This problem can be addressed, for example, by measuring correlations of photoluminescence intensity under conditions facilitating the supposed exciton condensation. Because the exciton condensation occurs in lateral domains associated with large-scale fluctuations in a chaotic potential, studies of photoluminescence in isolated domains by microprobe optical microscopy are of special interest. It is expected that under IWE condensation conditions, the photoluminescence of a single condensate-containing domain must be completely circularly polarized. In addition, in the case of weak interdomain bonding, time-related fluctuations of the circular polarization degree (the optical analog of the Josephson effect) can be expected.

I thank A V Larionov, A V Gorbunov, A A Dremin, S V Dubonos, and V E Bisti for their collaboration and V D Kulakovskii, I V Kukushkin, Yu M Kagan, Yu E Lozovik, S V Iordanskii, R A Suris, and G M Eliashberg for stimulating discussions.

References

1. Moskalenko S A *Fiz. Tverd. Tela* **4** 276 (1962) [*Sov. Phys. Solid State* **4** 199 (1962)]
2. Blatt J M, Böer K W, Brandt W *Phys. Rev.* **126** 1691 (1962)
3. Casella R C *J. Appl. Phys.* **34** 1703 (1963)
4. Keldysh L V, Kopaev Yu V *Fiz. Tverd. Tela* **6** 2791 (1964) [*Sov. Phys. Solid State* **6** 2219 (1965)]
5. Keldysh L V, Kozlov A N *Zh. Eksp. Teor. Fiz.* **54** 978 (1968) [*Sov. Phys. JETP* **27** 521 (1968)]
6. Kozlov A N, Maksimov L A *Zh. Eksp. Teor. Fiz.* **48** 1184 (1965) [*Sov. Phys. JETP* **21** 790 (1965)]
7. Comte C, Nozieres P *J. Phys.* (Paris) **43** 1069, 1083 (1982)
8. Anderson M H et al. *Science* **269** 198 (1995); Davis K B et al. *Phys. Rev. Lett.* **75** 3969 (1995)
9. Bradley C C et al. *Phys. Rev. Lett.* **75** 1687 (1995)
10. Jin D S et al. *Phys. Rev. Lett.* **77** 420 (1996)
11. Ketterle W, van Druten N J *Phys. Rev. A* **54** 656 (1996)
12. Keldysh L V, in *Trudy IX Mezhdunarodnoĭ Konf. po Fizike Poluprovodnikov, Moskva, 23–29 Iyulya 1968 g.* (Abstracts of IX Intern. Conf. on Physics of Semiconductors, Moscow, 23–29 July 1968) Vol. 2 (Moscow, 1968) p. 384
13. Jeffries C D, Keldysh L V (Eds) *Electron-Hole Droplets in Semiconductors* (Modern Problems in Condensed Matter Sciences, Vol. 6) (Amsterdam: North-Holland, 1983)
14. Rashba E I, Sturge M D (Eds) *Excitons* (Modern Problems in Condensed Matter Sciences, Vol. 2) (Amsterdam: North-Holland, 1982)
15. Hulin D, Mysyrowicz A, Benoît à la Guillaume C *Phys. Rev. Lett.* **45** 1970 (1980); Snoke D W, Wolfe J P, Mysyrowicz A *Phys. Rev. B* **41** 11171 (1990); Fortin E, Fafard S, Mysyrowicz A *Phys. Rev. Lett.* **70** 3951 (1993); Mysyrowicz A et al. *Solid State Commun.* **92** 957 (1994); Mysyrowicz A, Benson E, Fortin E *Phys. Rev. Lett.* **77** 896 (1996); **78** 3226 (1997)
16. Kukushkin I V, Kulakovskiĭ V D, Timofeev V B *Pis'ma Zh. Eksp. Teor. Fiz.* **34** 36 (1981) [*JETP Lett.* **34** 34 (1981)]; Timofeev V B, Kulakovskii V D, Kukushkin I V *Physica B+C* **117–118** 327 (1983)
17. O'Hara K E, Ó Súilleabháin L, Wolfe J P *Phys. Rev. B* **60** 10565 (1999); O'Hara K E, Wolfe J P *Phys. Rev. B* **62** 12909 (2000)
18. Kopelevich G A, Tikhodeev S G, Gippius N A *Zh. Eksp. Teor. Fiz.* **109** 2189 (1996) [*JETP* **82** 1180 (1996)]
19. Lozovik Yu E, Yudson V I *Pis'ma Zh. Eksp. Teor. Fiz.* **22** 556 (1975) [*JETP Lett.* **22** 274 (1975)]
20. Shevchenko S I *Fiz. Nizk. Temp.* **2** 505 (1976) [*J. Low Temp. Phys.* **2** 251 (1976)]
21. Fukuzawa T, Mendez E E, Hong J M *Phys. Rev. Lett.* **64** 3066 (1990)
22. Golub J E et al. *Phys. Rev. B* **41** 8564 (1990)
23. Kash J A et al. *Phys. Rev. Lett.* **66** 2247 (1991)
24. Butov L V et al. *Phys. Rev. Lett.* **73** 304 (1994)
25. Butov L V, in *Proc. of the 23th Intern. Conf. on the Physics of Semiconductors, Berlin, Germany, July 21–26, 1996* (Eds M Scheffer, R Zimmermann) (Singapore: World Scientific, 1996)
26. Timofeev V B et al. *Europhys. Lett.* **41** 535 (1998)
27. Timofeev V B et al. *Pis'ma Zh. Eksp. Teor. Fiz.* **67** 580 (1998) [*JETP Lett.* **67** 613 (1998)]
28. Krivolapchuk V V et al. *Solid State Commun.* **111** 49 (1999)
29. Butov L V et al. *Phys. Rev. B* **59** 1625 (1999)
30. Larionov A V et al. *Pis'ma Zh. Eksp. Teor. Fiz.* **117** 1255 (2000) [*JETP Lett.* **90** 1093 (2000)]
31. Butov L V et al. *Phys. Rev. B* **62** 1548 (2000)
32. Larionov A V et al. *Pis'ma Zh. Eksp. Teor. Fiz.* **75** 233 (2002) [*JETP Lett.* **75** 200 (2002)]
33. Ivanov A L, Ell C, Haug H *Phys. Rev. E* **55** 6363 (1997)
34. Ivanov A L, Littlewood P B, Haug H *Phys. Rev. B* **59** 5032 (1999)
35. Hohenberg P C *Phys. Rev.* **158** 383 (1967)
36. Mermin N D, Wagner H *Phys. Rev. Lett.* **17** 1133 (1966)
37. Kosterlitz J M, Thouless D J *J. Phys. C: Solid State Phys.* **6** 1181 (1973)

38. Zhu X et al. *Phys. Rev. Lett.* **74** 1633 (1995)
39. Yoshioka D, MacDonald A H *J. Phys. Soc. Jpn.* **59** 4211 (1990)
40. Chen X M, Quinn J J *Phys. Rev. Lett.* **67** 895 (1991)
41. Fernández-Rossier J, Tejedor C *Phys. Rev. Lett.* **78** 4809 (1997)
42. Lozovik Yu E, Berman O L *Zh. Eksp. Teor. Fiz.* **111** 1879 (1997) [*JETP* **84** 1027 (1997)]
43. Liu L, Świerkowski L, Neilson D *Physica B* **249 – 251** 594 (1998)
44. Lozovik Yu E, Ovchinnikov I V *Pis'ma Zh. Eksp. Teor. Fiz.* **74** 318 (2001) [*JETP Lett.* **74** 288 (2001)]
45. Larionov A V et al. *Pis'ma Zh. Eksp. Teor. Fiz.* **75** 689 (2002) [*JETP Lett.* **75** 570 (2002)]
46. Dremin A A et al. *Pis'ma Zh. Eksp. Teor. Fiz.* **76** 526 (2002) [*JETP Lett.* **76** 450 (2002)]
47. Timofeev V B et al. *Phys. Rev. B* **60** 8897 (1999)
48. Gorbunov A V, Timofeev V B, Bisti V E *Zh. Eksp. Teor. Fiz.* (2005) (in press)
49. Gorbunov A V, Timofeev V B *Pis'ma Zh. Eksp. Teor. Fiz.* **80** 210 (2004) [*JETP Lett.* **80** 185 (2004)]
50. Butov L V, Gossard A C, Chemla D S *Nature* **418** 751 (2002)
51. Butov L V et al. *Phys. Rev. Lett.* **92** 117404 (2004)
52. Snoke D et al. *Nature* **418** 754 (2002); Snoke D *Science* **298** 1368 (2002)
53. Rapaport R et al. *Phys. Rev. Lett.* **92** 117405 (2004)
54. Lerner I V, Lozovik Yu E *Zh. Eksp. Teor. Fiz.* **78** 1167 (1980) [*Sov. Phys. JETP* **51** 588 (1980)]
55. Butov L V et al. *Phys. Rev. Lett.* **87** 216804 (2001)
56. Lozovik Yu E et al. *Phys. Rev. B* **65** 235304 (2002)

PACS numbers: **42.65. – k**, **71.36. + c**, **78.65. – n**
DOI: 10.1070/PU2005v048n03ABEH002125

Hard excitation of stimulated polariton – polariton scattering in semiconductor microcavities

N A Gippius, S G Tikhodeev,
L V Keldysh, V D Kulakovskii

In recent years, unusual properties of polariton – polariton scattering of light in semiconductor microcavities have attracted continual attention [1 – 12]. In particular, it has been shown in experiment [13] [1] that as the resonant excitation frequency departs from the inflection point of the lower polariton branch (LPB), the scattered signal above the stimulated scattering threshold is always directed roughly perpendicularly to the microcavity (MC) plane. However, based on the simple four-wave mixing model [7], the signal should be expected to shift along the lower polariton branch (see the scattering diagram in Fig. 1).

This inference has recently been confirmed in [15]. Such behavior was theoretically explained in Refs [16 – 19] in terms of the interplay between two instabilities: bistability of the response of the polariton mode to an external pump and the parametric instability of this mode relative to the decay into scattered polaritons. The bistability of the linear optical response when the pump is normal to the surface of the microcavity (in the region of the LPB minimum) was demonstrated in a recent work [20]. However, the mutual influence of bistability and parametric instability feasible in the case of pump near the inflection point of the LPB gives rise to totally new and unexpected nonlinear effects. The aim of this paper is to discuss the physical interpretation of the instabilities found in Refs [16 – 19] and to analyze effects of quasi-two-dimensionality of polariton – polariton scattering and the saturation of excitonic transitions. We emphasize that from the quantum standpoint, macro-occupied polariton modes whose behavior is considered below obey the Bose statistics. Hence, we actually discuss the kinetics of a strongly nonequilibrium Bose system.

It is widely accepted that stimulated scattering commences softly (in analogy with the soft generator excitation regime) as the system loses stability for certain scattered modes when the threshold is exceeded. Such modes become macro-occupied as the threshold is passed over smoothly, and their amplitude gradually increases with the pump. Because the macro-occupied modes grow slowly (due to a small growth increment of unstable modes near the threshold), they effectively suppress the accumulation of the scattered signal in the nearby modes with a smaller incremental growth. Simultaneously, the pump mode amplitude is stabilized by the incoming energy balance. Such behavior is reminiscent of a *second*-order phase transition that occurs in a nonequilibrium system under the effect of external excitation, when the entire system passes concertedly and smoothly to a more stable macroscopic state.

Studies [17 – 19] have demonstrated that stimulated scattering of excitonic polaritons in a semiconductor MC can arise in a 'hard' manner (by analogy to the hard generator excitation regime). In this case, the amplitude of an *excited* polariton mode initially increases in a jump due to its bistability typical of nonlinear oscillators. If such transformation of the excited mode results in the system falling in the region of strong instability with respect to polariton – polariton scattering (or any other scattering, e.g., on phonons or free carriers), the corresponding modes in a large phase space region are characterized by substantial growth increments and start to be populated explosively. The incoming energy balance makes the population of the excited mode decrease abruptly, and the scattered signal is strongly stochastic. This behavior is similar to the *first*-order phase transition that occurs in a nonequilibrium system excited from the outside. Although the system in Refs [17 – 19] is assumed to be spatially uniform, one can expect its stratification into spatially inhomogeneous regions. It is worth noting that the bistability-allowed possibility of the nonlinear spatially inhomogeneous self-organization of the scattered signal has recently been considered theoretically in the framework of a similar approach in Ref. [21]. The same approach was applied in another recent work [22] to clarify the feasibility of superfluidity in the polariton system in a microcavity.

The process of polariton parametric scattering is illustrated by Fig. 1. The theoretical analysis of its development includes the consideration of semiclassical equations for $\mathcal{E}_{\mathrm{QW}}$, the quantum well (QW) electric field in a microcavity, and for the exciton polarization $\mathcal{P}(k,t)$ averaged over the QW width [19]:

$$\left[\mathrm{i}\frac{\mathrm{d}}{\mathrm{d}t} - E_{\mathrm{C}}(k)\right]\mathcal{E}_{\mathrm{QW}}(k,t) = \alpha(k)\mathcal{E}_{\mathrm{ext}}(k,t) + \beta(k)\mathcal{P}(k,t)\,, \quad (1)$$

$$\left[\mathrm{i}\frac{\mathrm{d}}{\mathrm{d}t} - E_{\mathrm{X}}(k)\right]\mathcal{P}(k,t)$$

$$= A\sum_{q,q'}\left[\delta_{q,k} - V_{\mathrm{sat}}\mathcal{P}(q',t)\,\mathcal{P}^*(q+q'-k,t)\right]\mathcal{E}_{\mathrm{QW}}(q,t)$$

$$+ F\sum_{q,q'}\mathcal{P}(q',t)\,\mathcal{P}^*(q+q'-k,t)\,\mathcal{P}(q,t) + \xi(k,t)\,. \quad (2)$$

[1] See also the next report [14] in this issue.